Influence of magnetic field offsets on the resistance of magnetic barriers in two-dimensional electron gases: Experiment and simulations

S. Hugger, M. Cerchez, H. Xu, and T. Heinzel*

Heinrich-Heine-Universität, Universitätsstrasse 1, 40225 Düsseldorf, Germany

Strongly localized, magnetic field structures oriented perpendicular to two-dimensional electron gases, also known as magnetic barriers, are shifted in B space by homogeneous, perpendicular magnetic fields. The magnetoresistance across the barrier shows a characteristic asymmetric dip in the regime where the polarity of the homogeneous magnetic field is opposite to that of the magnetic barrier. The measurements are in quantitative agreement with semiclassical simulations, which reveal that the magnetoresistance originates from the interplay of snake orbits with $E \times B$ drift at the edges of the Hall bar and with elastic scattering.

I. INTRODUCTION

The transport properties of two-dimensional electron gases (2DEGs) in spatially varying magnetic fields show a rich phenomenology, and several interesting effects have been reported recently. For example, magnetic superlattices[1,2] show commensurability oscillations in the magnetotransport, while giant magnetoresistance effects have been found on one-dimensional magnetic arrays.[2] Also, a variety of single magnetic nanostructures have been investigated via their influence on the 2DEG, such as resistance resonances along magnetic edge states,[3] the experimental realization of magnetic waveguides,[4] or the demonstration of Hall sensing.[5,6] A magnetic nanostructure of elementary character, known as *single magnetic barrier* (MB), is formed by the highly localized perpendicular (z) component B_{fz} of the magnetic fringe field in a 2DEG below the edge of a ferromagnetic film magnetized in the transport (x) direction.[7–15] Alternatively, such a structure can be defined in a 2DEG with a graded step.[16] Various aspects of MBs have been studied in the past few years. The height of the MB can be conveniently tuned by in-plane magnetic fields, while their magnetoresistance is interpreted in a semiclassical picture,[9–17] within which electrons experience a deflection by B_{fz}, such that for a fixed Fermi energy, the angle of incidence determines whether the electrons get transmitted or reflected.[7,18] MBs in quantum wires, on the other hand, have attracted a lot of recent attention from theory. These studies have established the potential of MBs as tunable spin filters,[19–29] and predict the presence of Fano resonances.[30]

In all experiments reported so far, the resistance of MBs has been investigated as a function either of a magnetic field applied in the x direction or of the carrier density.[9–16] Therefore, the polarity of the total magnetic field in the z direction $B_z(x)$ is constant. A qualitatively different situation arises when $B_z(x)$ changes its sign across the MB, since other types of trajectories with a snake orbit character become possible.

In the present paper, we report the experimental implementation of such a magnetic barrier structure. It is generated by superimposing a homogeneous perpendicular magnetic field B_{hz} to $B_{fz}(x)$. This way, a MB of constant strength and shape is displaced along the B_z axis. The most interesting situation arises when B_{hz} partly compensates $B_{fz}(x)$, such that

lines of zero magnetic field along the y direction act as guiding centers for snake orbits. In this range, a pronounced dip of asymmetric shape in the magnetoresistance is observed. We explain this structure by an interplay of the conductance enhancement along the y direction due to snake orbits with both elastic scattering and $E \times B$ drifts at the edges of the Hall bar. Numerical simulations based on the Landauer-Büttiker model and the Kubo formalism substantiate this interpretation.

The outline of the paper is as follows: Section II is dedicated to the experimental results. An interpretation of the data with the help of simulations is given in Sec. III, followed by a summary in Sec. IV.

II. EXPERIMENTS

The experiments have been performed on a commercially available GaAs/Al$_x$Ga$_{1−x}$As heterostructure[31] with a 2DEG 65 nm below the surface. The sample geometry is shown in Fig. 1(a). The samples were prepared by optical lithography, followed by wet chemical etching for the definition of the Hall bar, or by metallization steps, respectively. Au/Ge Ohmic contacts were defined at source and drain contacts and at the voltage probes. A dysprosium (Dy) platelet with a
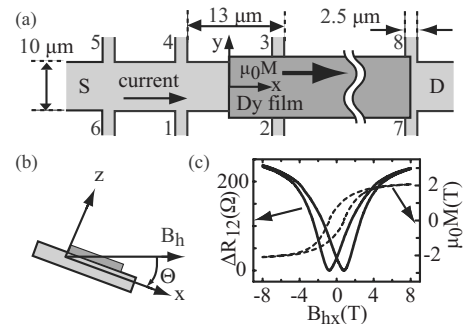

FIG. 1. (a) Top view of the schematic sample: a Dy platelet is placed on top of a Hall bar with source (S) and drain (D) contacts as well as voltage probes 1–8. (b) Nomenclature used for rotated samples. (c) The resistance $\Delta R_{12}(B_{hx})$ of the MB (the background resistance of the 2DEG is subtracted), measured at a temperature of 2 K, and the corresponding magnetization of the Dy film.
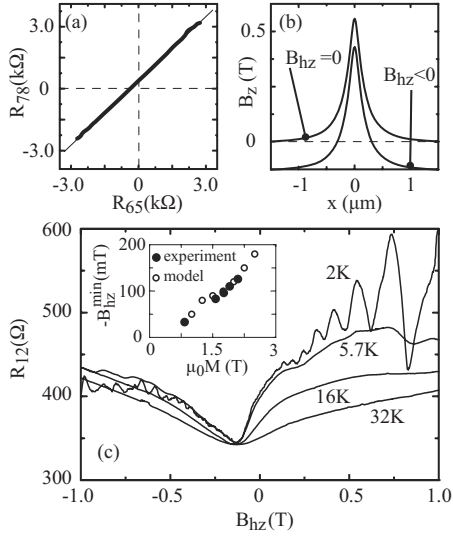
FIG. 2. (a) The Hall resistance R_{78} vs R_{65}, measured at 2 K (bold line), and the linear fit to the data (thin line), with a slope of 1.04. (b) Sketch of $B_z(x) = B_{fz}(x) + B_{hz}$ for $B_{hz} = 0$ and $B_{hz} = -125$ mT. (c) Measurements of $R_{12}(B_{hz})$. Inset: Measured and simulated values of B_{hz}^{min} as a function of the film magnetization.

thickness of 300 nm was deposited on the heterostructure surface by thermal evaporation at a base pressure of 2×10^{-6} mbar. A Cr/Au layer of 150 nm thickness was deposited on top to prevent the Dy from oxidizing under ambient conditions. The samples were measured in a liquid helium cryostat with a variable temperature insert. A rotatable sample stage allows orientation of the sample within the x-z plane [see Fig. 1(b)], with an accuracy of the rotation angle Θ of 0.1°. The cryostat is equipped with a superconductive magnet with a maximum homogeneous magnetic field of $B_h = 8$ T. A current of $I = 100$ nA with a frequency of 13 Hz was passed from source to drain. Conventional four-probe measurements as a function of perpendicular magnetic field B_{hz} were performed, from which an electron density of 2.45×10^{15} m^{-2} and a mobility of 22.1 m^2/V s (corresponding to a Drude scattering time of $\tau_D = 8.4$ ps and an elastic mean free path of 1.8 μm) were obtained at a temperature of 2 K. The quantum scattering time was determined from the envelope of the Shubnikov–de Haas oscillations[32] as $\tau_q = 1.04$ ps to an accuracy of 10%. The vanishing of the Hall voltage was used to adjust $\Theta = 0$.

In a previous publication, we have discussed in detail the resistance of such a MB as a function of a parallel magnetic field B_{hx}.[15] The fringe field $B_{fz}(x)$ is given by[12,18]

$$B_{fz}(x) = -\frac{\mu_0 M(B_{hx})}{4\pi} \ln\left(\frac{x^2 + z_0^2}{x^2 + (z_0 + h_0)^2}\right) \qquad (1)$$

[see Fig. 2(b)]. Here, z_0 is the distance of the 2DEG from the surface and h_0 denotes the thickness of the Dy film with a magnetization denoted by $M(B_{hx})$.

The MB was characterized by measuring its resistance R_{12} as a function of B_{hx} at $\Theta = 0$. Furthermore, from the fit of $R_{12}(B_{hx})$ to a semiclassical model,[15] the magnetization characteristics of the Dy film at its edge of relevance is obtained.

Five samples were measured, all with qualitatively identical behavior. Here, we focus on the sample with the strongest MB of $B_{fz}^{max} \equiv B_{fz}(x = 0) = 0.57$ T for $B_{hx} = 8$ T, corresponding to a saturation magnetization of $\mu_0 M_s = 2.1$ T.

With the MB established this way, we superimpose a homogeneous, perpendicular magnetic field B_{hz}. For this purpose, the sample is rotated at $B_h = 8$ T by small angles, such that the Dy film is kept at constant magnetization, while a homogeneous magnetic field in the z direction B_{hz} emerges [see Fig. 1(b)]. In Fig. 2(a), $R_{78}(B_{hz})$ is plotted as a function of $R_{65}(B_{hz})$. A linear relation with a slope of $dR_{78}/dR_{65} = 1.04$ and an offset of 380 Ω are found. Since both Hall crosses measure the average magnetic field in the probed section, we conclude that the MB is not modified by rotations in the range of interest, namely, for $|B_{hz}| \lesssim 1$ T, corresponding to $|\Theta| \lesssim 7.2°$. Thus, rotating the sample in this range corresponds to a displacement of $B_{fz}(x)$ along the B_z axis, as sketched in Fig. 2(b). Alternatively, we turned B_h off and set $\Theta = 90°$, in which case the MB originates from the remanence of the Dy film. In that setup, $|B_h| = |B_{hz}| \lesssim 0.2$ T can be applied without changing the film magnetization, which is kept in-plane by the shape anisotropy.

In Fig. 2(c), the magnetoresistance traces $R_{12}(B_{hz})$ at various temperatures are reproduced. A pronounced asymmetric dip of ≈ 90 Ω strength at 2 K, located at $B_{hz}^{min} = -125$ mT, is observed. As the temperature increases, the dip broadens, both its amplitude and its asymmetry are reduced, and the position of the minimum shifts slightly toward $B_{hz} = 0$, but the structure remains clearly visible at 32 K. The weak temperature dependence of the structure indicates a classical origin. In the inset of Fig. 2(c), B_{hz}^{min} is plotted as a function of the film magnetization, which is tuned by B_{hx}. B_{hz}^{min} drops approximately linearly as the magnetization is reduced. Furthermore, we notice a suppression of the Shubnikov–de Haas oscillations for $B_{hz} < 0$.

We remark that these asymmetries are distinctly different from those occasionally observed in 2DEGs as B_{hz} is inverted. We have measured, e.g., the longitudinal resistance between contacts 5 and 1, as well as between two contact underneath the Dy film (not shown). In both cases, ρ_{xx} shows a weakly pronounced maximum at $B_{hz} = 0$ and drops with slightly different slopes to the positive and the negative side of B_{hz}. In such measurements, the Shubnikov–de Haas amplitudes also deviate by a few percent as B_{hz} is inverted, but systematic or strong asymmetries are absent.

III. SIMULATION AND INTERPRETATION

An adequate model to simulate our system is the multiterminal Landauer-Büttiker formalism.[33,34] We have modeled a sample with sizes as shown in Fig. 1, including source and drain (which was set to zero potential) and voltage probes 1–4. The geometry with six contacts allows various consistency checks, e.g., simulations of the Hall effect outside the MB. The symmetry of the problem suggests the equivalence of the set of contacts {S,1,2} to {D,3,4}.

We inject 1.8×10^5 electrons at each cross-sectional line, defined at 2.5 μm inside the contacts S, 1, and 2. The electron positions on the injection lines and their injection angles
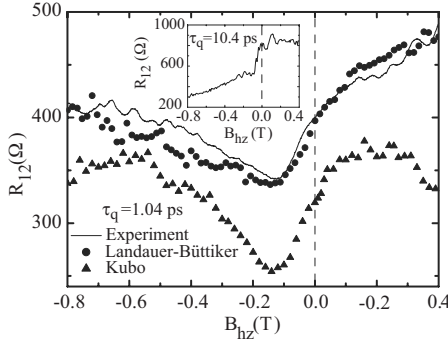
FIG. 3. Main figure: Comparison of the measured MB resistance as a function of B_{hz} (full line) with the results of simulations based on the Kubo model (triangles) and on the Landauer-Büttiker model (circles). The inset shows a simulation of $R_{12}(B_{hz})$ for the quasiballistic case as obtained within the Landauer-Büttiker model.

are random, while their kinetic energy equals the Fermi energy. We solve the equations of motion for the electrons and calculate their trajectories until they pass the cross-sectional line of any of the six contacts. The sample edges are simulated as hard walls with specular reflectivity. Elastic scattering is included by assuming small angle scattering with Gaussian distributed scattering angles (limited to the range $[-\pi, \pi]$) and Poisson distributed times between scattering events, with an expectation value equal to the measured τ_q. The full width at half maximum of the scattering angle distribution of 0.157π is given by the condition that the simulated value for τ_D has to agree with the experimentally determined one.[15]

Within the Landauer-Büttiker formalism, one finds

$$R_{12} = \frac{(V_1 - V_2)}{I} = (M^{-1})_{31} - (M^{-1})_{21}, \qquad (2)$$

where

$$M = \begin{bmatrix} G_S & -G_{S1} & -G_{S2} & -G_{S3} & -G_{S4} \\ -G_{1S} & G_1 & -G_{12} & -G_{13} & -G_{14} \\ -G_{2S} & -G_{21} & G_2 & -G_{23} & -G_{24} \\ -G_{3S} & -G_{31} & -G_{32} & G_3 & -G_{34} \\ -G_{4S} & -G_{41} & -G_{42} & -G_{4S} & G_4 \end{bmatrix}.$$

Here, the notation

$$G_j = \sum_{i \neq j} G_{ji}, \quad j = S, 1, 2, 3, 4; \quad i = S, 1, 2, 3, 4, D \qquad (3)$$

has been used. The individual components of the conductance tensor are given by

$$G_{ji} = \frac{2e^2}{h} N_i \cdot T_{ji}, \quad j, i = S, 1, 2, 3, 4. \qquad (4)$$

Here, T_{ji} denotes the transmission probability from contact i to contact j, and N_i is the number of modes in contact i.

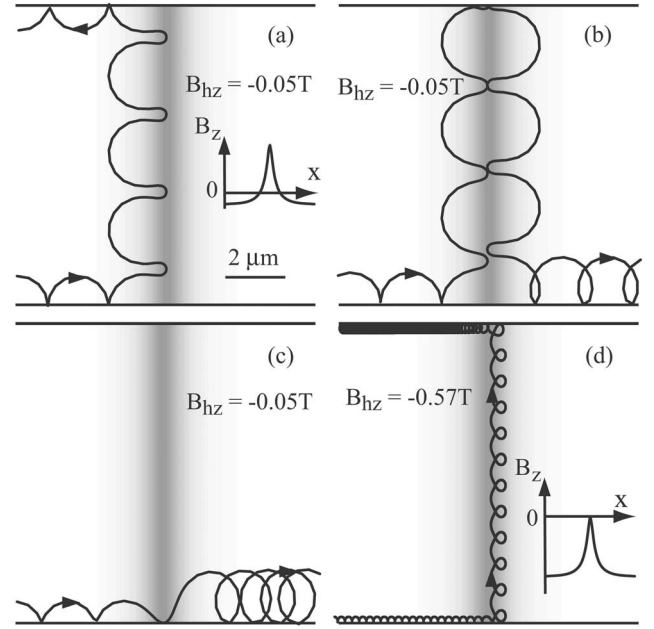The results of these simulations are reproduced in Fig. 3 in comparison to the experiment. We find good agreement

FIG. 4. Characteristic ballistic trajectories [(a)–(c)] within the dip region as well as for (d) $B_z(x) \lesssim 0$ for all x. $B_{fz}(x)$ is indicated in gray scale, while the corresponding $B_z(x)$ is sketched in the insets.

after a constant resistance of 12 Ω is added to the simulated trace of $R_{12}(B_{hz})$. This resistance originates from the parabolic magnetoresistivity of the 2DEG as a function of B_{hx} (Ref. 35) used to magnetize the Dy film in the experiment,[15] which at $B_{hx} \approx 8$ T amounts to the value taken into account. We emphasize that there is no fit parameter in this simulation. The simulated curve reproduces all classical aspects of the measurement, namely, the position of the minimum, the shape of the magnetoresistance dip, and the absolute values of the resistances. Similar agreement is obtained for other magnetizations, as indicated by the inset in Fig. 2(c), where the simulated B_{hz}^{min} is compared with the measured ones. We tentatively attribute the remaining deviations to distortions in the sample not considered in the model, such as nonspecular scattering and/or finite electric fields at the Hall bar edges, inhomogeneities of MB in the y direction, the spatial variations of B_{fx} as well as of the electron density across the MB, and thermal smearing.

We proceed by specifying the electron trajectories responsible for the enhanced conductance. In Fig. 4, characteristic ballistic trajectories starting from the source contact are shown for a MB with $B_{fz}^{max} = 0.57$ T.

For $B_{hz} > -80$ mT, the MB is closed, i.e., transmission is only possible via $E \times B$ drift at the edges of the Hall bar. In this regime, three scenarios for electrons entering the MB region exist, shown in Figs. 4(a)–4(c). Depending on the initial condition, i.e., the injection angle of the electron into the Hall bar, the electron either moves in snake-type orbits along the MB in the y direction [see Figs. 4(a) and 4(b)] or crosses the MB at the lower edge of the Hall bar [we denote those orbits as edge orbits, Fig. 4(c)]. At the upper edge, the snake orbits split into two groups. They either get reflected or transmitted, depending on the point where they hit the upper edge which determines the direction of the $E \times B$ drift.

As a result, a fraction of the trajectories that contribute to the enhancement of the conductance G_{yy} also participates in the transmission through the MB, thereby coupling G_{yy} to G_{xx}. Transport via edge orbits sets in at $B_{hz}=-50$ mT, and its weight increases as B_{hz} is made more negative. The snake orbits, on the other hand, are present in the interval $-B_{fz}^{max} < B_{hz} < 0$, in which $B_z(x)$ changes polarity. Their weights fluctuate, with an overall tendency to drop in the range where edge orbits exist. However, even for $B_{hz} \lesssim -B_{fz}^{max}$, the MB has an enhanced conductance in the y direction, due to orbits of the type shown in Fig. 4(d). Here, the magnetic field gradient at the MB leads to enhanced backscattering, which may be the reason why the Shubnikov–de Haas oscillations are suppressed at negative B_{hz}.

We have calculated $R_{12}(B_{hz})$ for a quasiballistic case with a rather high quantum scattering time, namely, $\tau_q=10.4$ ps, which could, nonetheless, be realized experimentally with high mobility heterostructures. The result is shown in the inset of Fig. 3. A *step* rather than a dip in R_{12} is obtained at the onset of edge orbits across the MB, at which the resistance drops by a factor of about 2. Moreover, in the regime where snake orbits are present, reproducible resistance fluctuations are found, which reflect the varying weight of those trajectories. A detailed discussion of these features is beyond the scope of this work. We note that at lower mobilities, scattering between various snake orbits smears the simulated resistance fluctuations.

Even though these simulations agree excellently with the data, a complementary, yet only qualitative, interpretation within the Kubo model[36] provides further insight, in particular, regarding the role of scattering, the position of the resistance minimum, and the relation to our experiments to those on one-dimensional magnetic superlattices. The Kubo formalism relates the components σ_{ij} ($\{i,j\}=\{x,y\}$) of the conductivity tensor to the electron velocity correlation functions $\langle v_i(t)v_j(0)\rangle$ by

$$\sigma_{ij} = \frac{m^* e^2}{\pi \hbar^2} \int_0^\infty \langle v_i(t)v_j(0)\rangle dt. \tag{5}$$

Here, the angle brackets denote averaging over all trajectories,[37] and $m^*=0.067m_e$ is the effective electron mass in GaAs. Since the formalism yields conductivities, its application to a single MB is not meaningful. Therefore, following Kubrak *et al.*,[38] we first consider a periodic array of MBs, each given by Eq. (1), and then calculate the resistance per barrier. This technique suffers from the difficulty of determining the appropriate value for the period a, which has been interpreted as an *active length*[38] of the MB. For the simulations, we used $a=2.5$ μm, i.e., such that one period contains 90% of the integrated magnetic field of a single MB. The trajectories of 10^5 electrons with the Fermi energy, injected in arbitrary directions at $y=0$ and arbitrary x within one lattice period, are calculated numerically to a length of 31 μm. Elastic scattering is included as described above.

In Fig. 5, we show the simulated functions $\sigma_{ij}(B_{hz})$. They have shapes resembling those obtained within the Boltzmann model, from which they deviate in three respects. First, the $\sigma_{ij}(B_{hz})$ traces are displaced in the B_z direction by $-\langle B_{fz}\rangle$, the
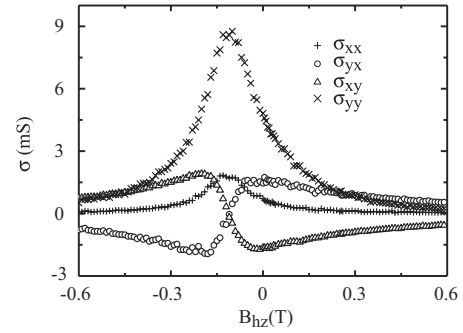

FIG. 5. Components of the conductivity tensor for a periodic array of MBs, as simulated within the Kubo model.

average fringe field in one period, and thus, centered at vanishing average magnetic field, $\langle B_z\rangle=0$. Second, the conductivities are scaled in the B_{hz} and in the σ_{ij} direction, with a particularly strong enhancement of σ_{yy} as compared to σ_{xx}. Finally, all σ_{ij} are asymmetric around $\langle B_z\rangle=0$. This is most clearly visible in the off-diagonal elements, the extremal values of which for $\langle B_z\rangle>0$ are significantly smaller than those for $\langle B_z\rangle<0$. To compare these simulations with the measurements, we use

$$R_{12} = (\rho_{xx} - \rho_0)\frac{a}{W} + \frac{L}{W}\rho_0, \tag{6}$$

where L denotes the distance between the voltage probes, W the width of the Hall bar, and ρ_0 the resistivity of the 2DEG in zero magnetic field. ρ_{xx} is given by

$$\rho_{xx} = \frac{\sigma_{yy}}{\sigma_{xx}\sigma_{yy} - \sigma_{xy}\sigma_{yx}}. \tag{7}$$

Figure 3 shows that the simulated magnetoresistance, albeit too low, agrees reasonably with the measured one in terms of magnitude and shape of the dip. The asymmetry is also visible, although less pronounced than in the experiments. The position of the simulated minimum corresponds to $\langle B_z\rangle=0$. We note that the simulated trace of $\rho_{yy}(B_{hz})$ remains basically unaffected by the MBs, while $\rho_{xy}(\langle B_z\rangle)=-\langle B_z\rangle/ne$ (not shown). Moreover, the results for ρ_{xx} are only weakly dependent on a for 2 μm $\leq a \leq 3$ μm. It is well known that periodic, one-dimensional superstructures (the homogeneous direction being the y direction) in 2DEGs can increase the diffusion in the y direction, which leads to a positive magnetoresistance $\rho_{xx}(B_z)$ around $B_z=0$.[2,39,40] The situation in our experiments is different, since (i) $\langle B_{fz}\rangle \neq 0$, and (ii) $B_{fz}(x)$ is asymmetric about $\langle B_z\rangle=0$. While the first point causes a simple displacement of $\rho_{xx}(B_{hz})$ in the B_{hz} direction, the second one generates asymmetries in $\rho_{xx}(B_{hz})$. In particular, $-\sigma_{xy}\sigma_{yx}(|\langle B_z\rangle|)<-\sigma_{xy}\sigma_{yx}(-|\langle B_z\rangle|)$ which, according to Eq. (7), increases $\rho_{xx}(|\langle B_z\rangle|)$ as compared to $\rho_{xx}(-|\langle B_z\rangle|)$. From this point of view, our experiments on single MBs are complementary to previous studies on periodic one-dimensional magnetic superlattices with vanishing average magnetic field, where both a positive magnetoresistance around $B=0$ and commensurability oscillations at higher

magnetic fields have been found.[1,2] Apparently, the positive magnetoresistance does not require a periodic structure and the related commensurate orbits, but rather emerges already from a single unit cell of the superlattice.

IV. SUMMARY AND CONCLUSIONS

The resistance of a magnetic barrier as a function of superimposed, homogeneous perpendicular magnetic fields has been investigated both experimentally and theoretically. The magnetoresistance shows a characteristic asymmetric dip at a homogeneous magnetic field of opposite direction to that of the barrier. Simulations show that electrons can travel along the barrier in snake orbits as well as in cyclotron-type orbits with magnetic-field-gradient-induced drifting centers. At the sample edges, edge orbits exist due to $E \times B$ drifts. They effectively couple G_{yy} to G_{xx}, thereby reducing the resistance of the magnetic barrier. The observed asymmetric resistance dip is interpreted in terms of the combined effects of (i) enhancement of G_{yy}, (ii) transmission via edge orbits, and (iii) elastic scattering in the barrier region. Simulations based on the multiterminal Landauer-Büttiker model without adjustable parameters result in excellent agreement with the experiment. In addition, they predict parametric resistance fluctuations in the regime of small homogeneous perpendicular magnetic fields, which will be interesting to study experimentally in further work.

ACKNOWLEDGMENTS

*thomas.heinzel@uni-duesseldorf.de

[1] P. D. Ye, D. Weiss, R. R. Gerhardts, M. Seeger, K. von Klitzing, K. Eberl, and H. Nickel, Phys. Rev. Lett. **74**, 3013 (1995).

[2] A. Nogaret, S. Carlton, B. L. Gallagher, P. C. Main, M. Henini, R. Wirtz, R. Newbury, M. A. Howson, and S. P. Beaumont, Phys. Rev. B **55**, R16037 (1997).

[3] A. Nogaret, S. J. Bending, and M. Henini, Phys. Rev. Lett. **84**, 2231 (2000).

[4] A. Nogaret, D. N. Lawton, D. K. Maude, J. C. Portal, and M. Henini, Phys. Rev. B **67**, 165317 (2003).

[5] F. M. Peeters and X. Q. Li, Appl. Phys. Lett. **72**, 572 (1998).

[6] K. S. Novoselov, A. K. Geim, S. V. Dubonos, Y. G. Cornelissens, F. M. Peeters, and J. C. Maan, Phys. Rev. B **65**, 233312 (2002).

[7] F. M. Peeters and A. Matulis, Phys. Rev. B **48**, 15166 (1993).

[8] A. Matulis, F. M. Peeters, and P. Vasilopoulos, Phys. Rev. Lett. **72**, 1518 (1994).

[9] F. G. Monzon, M. Johnson, and M. L. Roukes, Appl. Phys. Lett. **71**, 3087 (1997).

[10] M. Johnson, B. R. Bennett, M. J. Yang, M. M. Miller, and B. V. Shanabrook, Appl. Phys. Lett. **71**, 974 (1997).

[11] V. Kubrak, A. C. Neumann, B. L. Gallagher, P. C. Main, and M. Henini, J. Appl. Phys. **87**, 5986 (2000).

[12] T. Vančura, T. Ihn, S. Broderick, K. Ensslin, W. Wegscheider, and M. Bichler, Phys. Rev. B **62**, 5074 (2000).

[13] B. L. Gallagher, V. Kubrak, A. W. Rushforth, A. C. Neumann, K. W. Edmonds, P. C. Main, M. Henini, C. H. Marrows, B. J. Hickey, and S. Thoms, Physica E (Amsterdam) **11**, 171 (2001).

[14] V. Kubrak, K. W. Edmonds, A. C. Neumann, B. L. Gallagher, P. C. Main, M. Henini, C. H. Marrows, B. J. Hickey, and S. Thoms, IEEE Trans. Magn. **37**, 1992 (2001).

[15] M. Cerchez, S. Hugger, T. Heinzel, and N. Schulz, Phys. Rev. B **75**, 035341 (2007).

[16] M. L. Leadbeater, C. L. Foden, J. H. Burroughes, M. Pepper, T. M. Burke, L. L. Wang, M. P. Grimshaw, and D. A. Ritchie, Phys. Rev. B **52**, R8629 (1995).

[17] J. Hong, V. Kubrak, K. W. Edmonds, A. C. Neumann, B. L. Gallagher, P. C. Main, M. Henini, C. H. Marrows, B. J. Hickey, and S. Thoms, Physica E (Amsterdam) **12**, 229 (2002).

[18] I. S. Ibrahim, V. A. Schweigert, and F. M. Peeters, Phys. Rev. B **56**, 7508 (1997).

[19] A. Majumdar, Phys. Rev. B **54**, 11911 (1996).

[20] Y. Guo, B. L. Gu, Z. Zeng, J. Z. Yu, and Y. Kawazoe, Phys. Rev. B **62**, 2635 (2000).

[21] G. Papp and F. M. Peeters, Appl. Phys. Lett. **78**, 2184 (2001).

[22] G. Papp and F. M. Peeters, Appl. Phys. Lett. **79**, 3198 (2001).

[23] H. Z. Xu and Y. Okada, Appl. Phys. Lett. **79**, 3119 (2001).

[24] M.-W. Lu, L.-D. Zhang, and X.-H. Yan, Phys. Rev. B **66**, 224412 (2002).

[25] Y. Guo, Z. Feng, B. L. Gu, and Y. Kawazoe, Phys. Rev. B **66**, 045312 (2002).

[26] Y. Jiang, M. B. A. Jalil, and T. Low, Appl. Phys. Lett. **80**, 1673 (2002).

[27] W. Xu and Y. Guo, Phys. Lett. A **340**, 281 (2005).

[28] F. Zhai and H. Q. Xu, Phys. Rev. B **72**, 085314 (2005).

[29] F. Zhai and H. Q. Xu, Appl. Phys. Lett. **88**, 032502 (2006).

[30] H. Xu, T. Heinzel, M. Evaldsson, S. Ihnatsenka, and I. V. Zozoulenko, Phys. Rev. B **75**, 205301 (2007).

[31] The heterostructures have been purchased from Intelligent Epitaxy Tech., Richardson, TX, USA.

[32] T. Ando, A. B. Fowler, and F. Stern, Rev. Mod. Phys. **54**, 437 (1982).

[33] M. Büttiker, Phys. Rev. Lett. **57**, 1761 (1986).

[34] C. W. J. Beenakker and H. van Houten, Phys. Rev. Lett. **63**, 1857 (1989).

[35] P. A. Lee and T. V. Ramakrishnan, Rev. Mod. Phys. **57**, 287 (1985).

[36] R. Kubo, J. Phys. Soc. Jpn. **12**, 570 (1957).

[37] K. Richter, *Semiclassical Theory of Mesoscopic Quantum Systems* (Springer, New York, 2004).

[38] V. Kubrak, F. Rahman, B. L. Gallagher, P. C. Main, M. Henini, C. H. Marrows, and M. A. Howson, Appl. Phys. Lett. **74**, 2507 (1999).

[39] C. W. J. Beenakker, Phys. Rev. Lett. **62**, 2020 (1989).

[40] P. H. Beton, E. S. Alves, P. C. Main, L. Eaves, M. W. Dellow, M. Henini, O. H. Hughes, S. P. Beaumont, and C. D. Wilkinson, Phys. Rev. B **42**, 9229 (1990).